AN-04-6-2

Methods for Calculating the Effective Longwave Radiative Properties of a Venetian Blind Layer

Darryl S. Yahoda

John L. Wright, Ph.D., P.Eng.
Member ASHRAE

ABSTRACT

Window solar gain can strongly influence building energy consumption, peak loads, and comfort. Shading devices are routinely used to control solar gain. The use of venetian blinds is particularly common. There is a strong need for models that can accurately simulate this type of device. As a first step, this study deals with the mechanisms of longwave radiant exchange. Methods are presented by which spatially averaged optical properties (referred to as "effective" optical properties) can be calculated. An enclosure model was formulated to model the interaction of radiation with the slat surfaces. Six enclosure areas, rather than four, were used to account for the possible overlap of blind slats. This optical model allows the venetian blind to be treated as a planar, homogeneous "black-box" layer in a series of glazing layers and, coupled with the appropriate convection model, can be incorporated within a standard one-dimensional center-glass heat transfer analysis. Sample calculations were performed and the resulting effective optical properties discussed. The model compares favorably with expected trends and limits. The effect of slat curvature was also examined.

INTRODUCTION

One strategy for reducing solar heat gain through windows is the use of a slat-type shading device—in particular, a venetian blind—that can act as an adjustable barrier to solar transmission. The selection of the correct shading system requires information on the optical characteristics of the shading system as well as its influence on heat transfer. This selection process is complicated by the myriad available shading products, often with variable geometries, and the inability of current evaluation and rating techniques, based on one-dimensional center-glass computer analysis, to accurately simulate shading systems. The result is that expensive and time-consuming calorimetric testing is the only alternative for assessing the thermal performance of shading systems.

Typically, the analysis of the center-glass area of glazing systems takes advantage of the fact that there is no appreciable overlap between the band of solar wavelengths (0.3 to 3 μm) and the band of longer wavelengths (3 to 50 μm) by which radiant transfer occurs. This absence of overlap between the solar and longwave spectra allows the analysis to be carried out in two steps. First, a solar-optical calculation determines how much solar radiation is absorbed at each layer and how much is transmitted to the indoor space. Second, a heat transfer analysis is used to perform an energy balance at each layer in which the net heat transfer from a layer must equal the amount of absorbed solar radiation (e.g., Wright 1998, Hollands et al. 2001). The simultaneous solution of the resulting set of energy balance equations yields the temperature of each glazing layer as well as the various values of heat flux and heat flux components at each location within the system.

In order to expand the scope of center-glass simulation, the front and back surfaces of the shading layer are assigned spatially averaged optical properties, called "effective" optical properties. The use of effective optical properties allows the shading layer to be treated as a homogeneous, planar layer within a glazing system. For example, the entire glazing system can be treated as an n-node array consisting of n-3 glazing layers, one shading layer, together with the indoor ($i = 1$) and outdoor ($i = n$) nodes, as shown in Figure 1.

A complete energy flow analysis requires the effective optical properties, both solar and longwave, of the shading layer. A number of models for radiation transport through

Darryl S. Yahoda is a consultant at DBM Systems, Inc., Cambridge, Ontario, Canada, and **John L. Wright** is Associate Professor in the Department of Mechanical Engineering, University of Waterloo, Waterloo, Ontario, Canada.

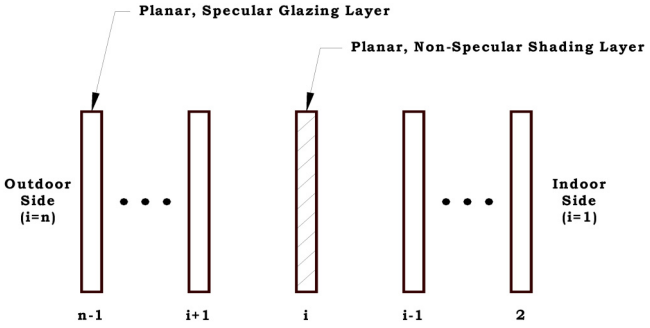

Figure 1 *Layer representation of glazing system with venetian blind.*

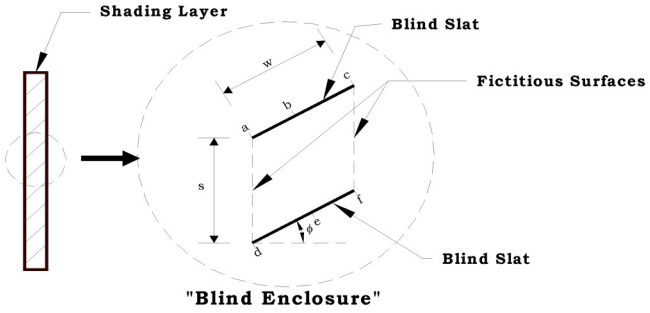

Figure 2 *"Blind enclosure" representative of blind layer.*

venetian blinds exist in the literature. Unfortunately, most are strictly concerned with solar radiation (e.g., Klems 1994a, 1994b, 2002). The models that do treat longwave radiant exchange (ISO 2000; Rheault and Bilgen 1989) are based on radiosity/irradiance calculations, similar to the models presented in this paper, but some similarities and differences should be noted. Both earlier models (ISO 2000; Rheault and Bilgen 1989) prescribe a subdivision of the slat surface by reusing the divisions used in the analysis of incident solar radiation. Rheault divides the slat according to the extent of direct-beam solar radiation, and the ISO model uses five slat segments of equal size. The model described here is focused solely on the longwave aspects of the analysis and decisions regarding slat surface subdivision are based only on the consideration of longwave radiation. Rheault and Bilgen (1989) do not present results in the form of effective optical properties, but a small set of effective transmittance and effective emissivity results is presented in the ISO (2000) document. The results presented for opaque venetian blind slats (slats that are not opaque with respect to longwave radiation are felt to be very rare) agree very closely with results produced using the model currently described—a preliminary indication that good results can be obtained for longwave analysis using far fewer than five slat divisions.

The purpose of this paper is to describe methods for determining the effective longwave radiative properties of the shading layer, which can be used in the heat transfer analysis of the glazing system. An effort has been made to retain a level of simplicity in these models that is expected to translate into ease of implementation. The models described are based on conventional gray enclosure analysis and, thus, entail the assumptions that each surface is isothermal, uniformly irradiated, and a diffuse reflector/emitter. The resulting effective longwave radiative properties of the blind layer are functions of the emissivity of the slat material and the blind geometry, which is composed of the angle of tilt of the slats (slat angle), ϕ, slat width, w, and the spacing between adjacent slats, s. Details regarding blind slat geometry are shown in Figure 2.

EFFECTIVE LONGWAVE RADIATIVE PROPERTIES

The radiant analysis of the shading layer is based on the assumptions that the blind slats are flat, have uniform, non-temperature-dependent properties, and are opaque with respect to longwave radiation. The slat material is also assumed to be gray and emit and reflect diffusely in the longwave spectrum. The blind slats are assumed to be long, allowing the geometry to be treated as two-dimensional.

Enclosure Geometry

The effective longwave radiative properties of the shading layer can be determined by examining an area of the layer that will be representative of the layer as a whole. For a venetian blind composed of a sufficiently large number of slats, the optical characteristics of the area between two adjacent slats will be representative of the entire layer. The two adjacent slat surfaces, with fictitious surfaces at the front and back openings, constitute an enclosure.

The blind enclosure is split into six surfaces: two fictitious surfaces represent the openings and each slat is divided into two surfaces, as shown in Figure 2. The surfaces are numbered as follows: surface 1 = ab, surface 2 = bc, surface 3 = de, surface 4 = ef, surface 5 = ad, and surface 6 = cf. The lengths of the slat subsurfaces (i.e., the locations of points b and e) depend on the ratio of slat width to slat spacing, w/s. When the slat angle, ϕ, is increased to 90°, the blind slats will be vertical and the blind is said to be in a "closed" position. Two situations, dependent on the w/s ratio, can arise when the blind is closed. If $w/s \leq 1$, there will be a gap between the adjacent slat ends (and radiation transmission can take place even though the blinds are closed) or the slats will be tip-to-tip for the case of $w/s = 1$. For $w/s \leq 1$, a four-surface enclosure is sufficient so point b is located coincident with the slat tip at point c, and point e is located coincident with the slat tip at point f. In other words, areas 2 and 4, bc and ef, respectively, vanish. Alternatively, if $w/s > 1$, the slats will overlap when the blind is closed. In this situation, no radiation transmission should occur. However, the use of a four-surface enclosure for $w/s > 1$ will produce a false transmittance, which will be discussed in

Table 1. Enclosure Line Segments Dependent on *w/s* Ratio

Line Segment	Length		
	w/s ≤ 1 (all ϕ)	**w/s > 1 (ϕ < 0°)**	**w/s > 1 (ϕ ≥ 0°)**
ab	w	s	w – s
bc	0	w – s	s
be	s	$\sqrt{s^2 + (2s-w)^2 - 2s(2s-w)\sin\lvert\phi\rvert}$	
bf	s	$\sqrt{s^2 + (bc)^2 - 2s(bc)\sin\phi}$	
ce	s	$\sqrt{s^2 + (ef)^2 - 2s(ef)\sin\phi}$	
de	w	w – s	s
ef	0	s	w – s

greater detail later, making a six-surface enclosure necessary to account for the slat overlap. In cases with $w/s > 1$, point b and point e are positioned to account for slat overlap. For positive slat angles, point b is positioned a distance s from point c, and point e is positioned a distance s from point d in order to have areas 1 and 4, ab and ef, respectively, represent the areas of slat overlap. For negative slat angles, point b is positioned a distance s from point a, and point e is positioned a distance s from point f in order to have areas 2 and 3, bc and de, respectively, represent the areas of slat overlap.

Enclosure View Factors

Since the blind enclosure is modeled as a two-dimensional system, the radiative view factor from surface i to surface j, F_{ij}, can be determined using Hottel's crossed string method (e.g., Siegel and Howell 1992). In general, to find the view factor from surface i to surface j, Hottel's crossed string method can be expressed as

$$F_{ij} = \frac{\sum XS_{ij} - \sum US_{ij}}{2L_i}, \quad (1)$$

where the string lengths are:

ΣXS_{ij} = the sum of the "crossed" strings joining the ith and jth surfaces,

ΣUS_{ij} = the sum of the "uncrossed" strings joining the ith and jth surfaces,

L_i = the length of ith surface.

The string lengths are determined by joining the end points of the two surfaces being examined using two "crossed" strings and two "uncrossed" strings. Table 1 lists the string lengths that are dependent on both the w/s ratio and the slat angle. The remaining line segment lengths can be determined using Table 2. The self-viewing factors, F_{ii}, will be zero because all surfaces are flat.

Table 2. Enclosure Line Segments for Use with All *w/s* Ratios

Line Segment	Length
ac	w
ad	s
ae	$\sqrt{s^2 + (de)^2 - 2s(de)\sin\phi}$
af	$\sqrt{s^2 + w^2 - 2ws\sin\phi}$
bd	$\sqrt{s^2 + (ab)^2 + 2s(ab)\sin\phi}$
cd	$\sqrt{s^2 + w^2 + 2ws\sin\phi}$
cf	s
df	w

Radiant Analysis

It is convenient for the enclosure analysis to be undertaken using an irradiance/radiosity formulation. The irradiance at surface i, G_i, is simply the radiant flux incident at that surface. The radiosity of surface i, J_i, is defined as the radiant flux leaving that surface.

Assuming that each surface is a diffuse emitter/reflector and that each surface is uniformly irradiated, it can be shown that the irradiance at the ith surface can be expressed in terms of the radiosities of all of the enclosure surfaces. In an n-surface enclosure (in this study, $n = 6$),

$$G_i = \sum_{j=1}^{n} F_{ij} J_j . \quad (2)$$

The radiosity at surface i includes the reflected portion of G_i as well as the radiant flux emitted by surface i itself.

$$J_i = \varepsilon_i \sigma T_i^4 + (1 - \varepsilon_i) G_i \quad (3)$$

where ε_i is the emissivity of surface i, σ is the Stefan-Boltzmann constant, and Kirchoff's law lets the surface reflectivity to be expressed as $(1 - \varepsilon_i)$.

Equations 2 and 3 were used to characterize the radiant exchange at surfaces 1 through 4—the blind slat surfaces. In calculating effective longwave transmittance, reflectance, and absorptance values, it is only necessary to follow the radiation that originates outside of the shading layer. That is, it is sufficient to follow the externally imposed radiation and note the portion that is transmitted through the shading layer, reflected from the shading layer, or absorbed at one of the slat surfaces. Therefore, the first term in the right-hand side of Equation 3 was set to zero for the purpose of estimating these effective properties.

The remaining enclosure surfaces, the openings to the enclosure, surfaces 5 and 6, transmit all incident radiation. Therefore, the radiosities of these surfaces, viewed from within the enclosure, include only radiation from a source external to the enclosure. To determine the front effective properties (FEP) of the shading layer, an irradiance, G_{front}, is imposed external to the front side of the enclosure on surface 5. A similar calculation is used to determine the back effective properties (BEP) of the shading layer by imposing an external irradiance, G_{back}, to the back side of the enclosure on surface 6. The radiosities and irradiances for the system are shown in Figure 3 for both the FEP and BEP cases. As noted in Figure 3, the radiosities for surface 5 and surface 6 are given by:

$$J_5 = G_{front} \quad \text{[FEP]} \qquad \text{or} \qquad J_5 = 0 \quad \text{[BEP]} \tag{4}$$

$$J_6 = 0 \quad \text{[FEP]} \qquad \text{or} \qquad J_6 = G_{back} \quad \text{[BEP]} \tag{5}$$

A system of ten equations and ten unknowns ($J_1, J_2, J_3, J_4, G_1, G_2, G_3, G_4, G_5, G_6$) arises from the application of Equations 2 through 5. Each emissivity used in Equation 3 (ε_1, ε_2, ε_3, and ε_4) is the total (longwave) hemispheric emissivity of an individual slat surface. It is clear that ε_1 must be equal to ε_2 and ε_3 must be equal to ε_4. The opposite sides of a slat can be assigned a different emissivity to account for dust accumulation or differing surface finishes.

Front and Back Effective Properties

Several methods can be used to determine the effective longwave properties for a venetian blind layer. Since the solution procedures are equally applicable for finding the front or back effective properties, the subscript k will be used in place of either *front* or *back*. Each method is based on the idea that an irradiance, G_{front} or G_{back}, is introduced from outside of the enclosure. The imposed irradiance, G_{front} or G_{back}, reaches the enclosure as either J_5 or J_6, respectively. To generalize, the imposed irradiance, G_{front} or G_{back}, will be called G_k. Since the areas of the two enclosure openings are equal, the area of incidence will be called A_k. Also, the emissivity pairs of ε_1, ε_2 and ε_3, ε_4 will be called ε_{top} and ε_{bottom}, respectively, in reference to the emissivities of the top and bottom slat surfaces of the enclosure. Using Kirchoff's law again, the slat absorptivity, α_i, is equal to the slat emissivity, ε_i.

Each effective property will be expressed in the form, $X_{k,eff,LW}$, where X can be α, ρ, or τ. The subscript has three components: k to denote whether it is a front or back property, *eff* to signify it as an effective property, and *LW* to denote its applicability to radiation transport in the longwave spectrum.

Effective Longwave Absorptance ($\alpha_{k,eff,LW}$)—Method 1

The fraction of the imposed irradiance, G_k, absorbed can be determined from an energy balance on the blind enclosure using the reasoning that the amount of supplied energy that is apparently absorbed by the "k" surface of the shading layer should be equal to the total amount of energy absorbed at the slat surfaces. The rate of energy supplied to the enclosure will be the product of G_k, and the area over which it is incident, A_k. The fraction of this irradiance absorbed in the blind enclosure is $\alpha_{k,eff,LW}$. The rate of absorption on a slat surface can be expressed in terms of the slat material's absorptivity ($\varepsilon_i = \alpha_i$) and the rate at which radiant energy arrives at that surface, $A_i G_i$. Recalling that the top slat surface is composed of surfaces 1 and 2 and the bottom slat surface is composed of surfaces 3 and 4, the corresponding energy balance is

$$\alpha_{k,eff,LW} A_k G_k = \varepsilon_{top}(A_1 G_1 + A_2 G_2) + \varepsilon_{bottom}(A_3 G_3 + A_4 G_4) . \tag{6}$$

Rearranging,

$$\alpha_{k,eff,LW} = \frac{\varepsilon_{top}(A_1 G_1 + A_2 G_2) + \varepsilon_{bottom}(A_3 G_3 + A_4 G_4)}{A_k G_k} . \tag{7}$$

Equation 7 represents one method for determining the effective longwave absorptance of the shading layer. It should be noted that $\alpha_{k,eff,LW}$ is independent of the magnitude of G_k, which will be divided out of the expression when the solved irradiances are substituted.

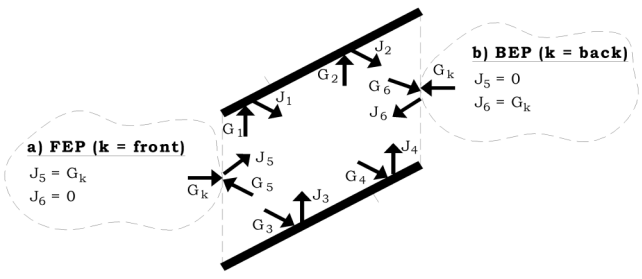

Figure 3 *Surface radiosities and irradiances for front and back effective properties.*

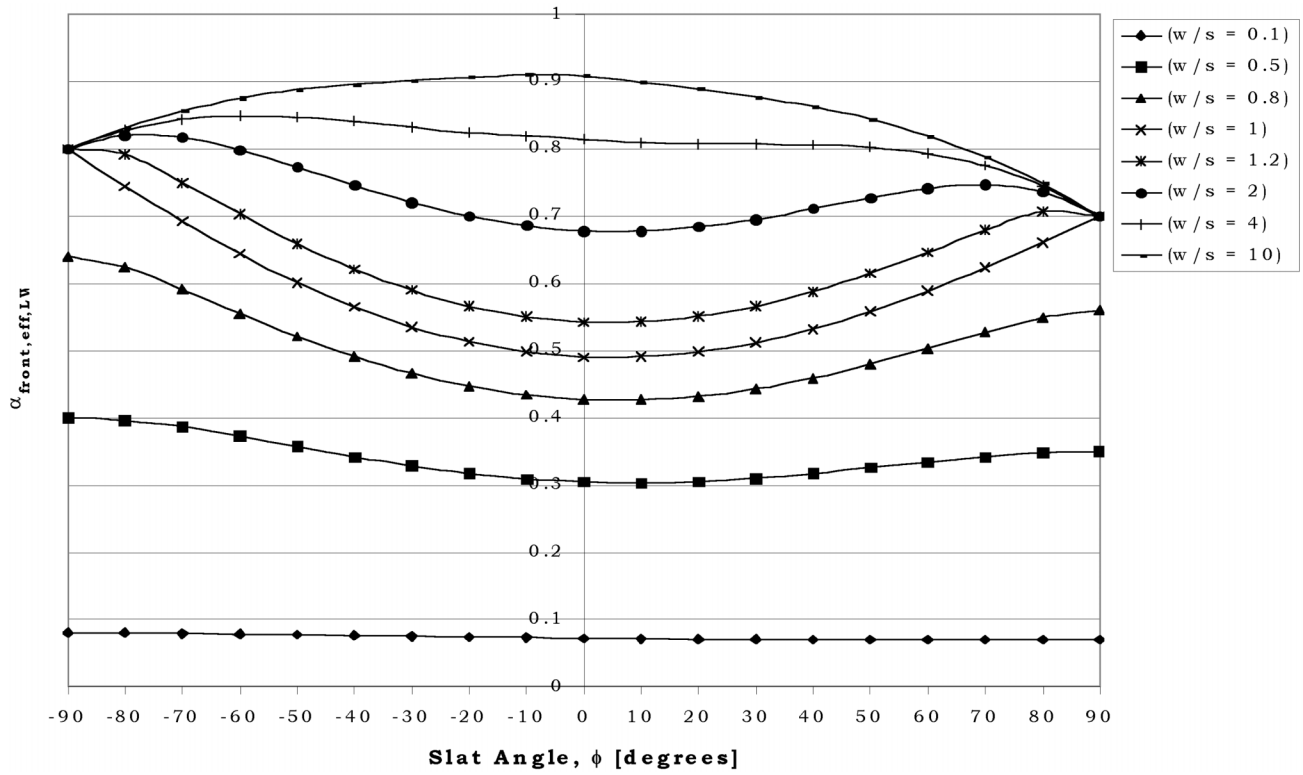

Figure 4 *Front effective longwave absorptance as a function of slat angle for various* w/s *ratios and* $\varepsilon_{top} = 0.8$, $\varepsilon_{bottom} = 0.7$.

Effective Longwave Absorptance ($\alpha_{k,eff,LW}$)—Method 2

The effective longwave absorptance of the shading layer can also be determined by noting that the fraction of G_k that is not transmitted or reflected must be absorbed. The rate at which energy escapes the shading layer will be equal to the sum of the irradiances on the opening surfaces multiplied by the areas of the respective openings; that is, $A_k G_5 + A_k G_6$. The rate of absorption will be equal to the rate at which energy is supplied to the enclosure less the rate at which energy is transmitted and reflected. Thus,

$$\alpha_{k,eff,LW} A_k G_k = A_k G_k - A_5 G_5 - A_6 G_6 \,. \tag{8}$$

Rearranging and simplifying, while noting that $A_k = A_5 = A_6$,

$$\alpha_{k,eff,LW} = 1 - \frac{(G_5 + G_6)}{G_k} \,. \tag{9}$$

Equation 9 represents a second method for determining the effective longwave absorptance of the shading layer. Again, it should be noted that $\alpha_{k,eff,LW}$ is independent of the magnitude of G_k, which will be divided out of the expression when the solved irradiances are substituted.

Effective Longwave Absorptance—Results

Figure 4 shows the effective front absorptance, $\alpha_{front,eff,LW}$, as a function of slat angle, ϕ, for different *w*/*s* ratios (slat width/slat spacing) and $\varepsilon_{top} = 0.8$ and $\varepsilon_{bottom} = 0.7$. Note that for $w/s \geq 1$, when the blind is completely closed ($\phi = \pm 90°$), the value of $\alpha_{front,eff,LW}$ is always equal to the absorptivity of slat surface facing the front of the enclosure. This should be expected.

For $w/s < 1$, $\alpha_{front,eff,LW}$ is less than the value of the slat surface absorptivity because even in the closed position, gaps will be present, allowing for transmission of radiation. The reduced absorptance should be expected from an inspection of Equation 7, which has the irradiance of each surface weighted by its respective area.

Although *w*/*s* ratios much greater than unity are not practical, it is instructive to observe that as the *w*/*s* ratio is increased to values much greater than unity, the effective absorptance will approach 100% when the blind is in the open position ($\phi = 0$). This should also be expected because as the *w*/*s* ratio becomes much greater than unity and $\phi = 0$, the slats will exchange radiation primarily with each other and "see" much less of the openings. This results in less transmission and reflectance because incident radiation cannot escape the cavity.

Effective Longwave Emittance ($\varepsilon_{k,eff,LW}$)

The effective longwave emittance of the shading layer can be determined from the rate at which the energy emitted by the slats leaves the enclosure through each opening. The ratio of energy leaving an opening—front or back—to the total energy emitted by the blind slats will yield the emittance for that given opening. Now the radiosity of each surface will be composed of the energy emitted by the surface plus the portion of irradiance that is reflected by the surface and both terms appearing in Equation 2 are retained. To determine $\varepsilon_{k,eff,LW}$, the slat temperature is left as a variable, T. It is again noted that the openings transmit all incident radiation but, for this situation, no external radiation is introduced. Hence, $J_5 = J_6 = 0$. Applying Equation 2 to every surface and Equation 3 to surfaces 1 through 4, a set of ten equations and ten unknowns (J_1, J_2, J_3, J_4, G_1, G_2, G_3, G_4, G_5, G_6) results.

The rate at which energy (emitted by the blind slats) emerges through side "k" of the enclosure will be equal to the product of the irradiance of the opening surface, G_5 (k = front) or G_6 (k = *back*), and A_k. The slat surfaces are assigned a uniform, arbitrary temperature. This allows the system of equations to be solved analytically or numerically. The rate of emitted energy can now be expressed in terms of the radiation a blackbody would emit at this temperature multiplied by the effective longwave emittance of the surface for side k. Equating these two expressions for the emitted energy for the front side results in

$$\varepsilon_{front,eff,LW}\sigma A_k T^4 = A_k G_5 , \tag{10}$$

and, for the back side,

$$\varepsilon_{back,eff,LW}\sigma A_k T^4 = A_k G_6 . \tag{11}$$

Rearranging and simplifying,

$$\varepsilon_{front,eff,LW} = \frac{G_5}{\sigma T^4} , \tag{12}$$

and, for the back side,

$$\varepsilon_{back,eff,LW} = \frac{G_6}{\sigma T^4} . \tag{13}$$

Equations 12 and Equation 13 represent a method for determining the effective longwave emittance for the front and back surfaces of the shading layer. Again, it should be noted that $\varepsilon_{front,eff,LW}$ and $\varepsilon_{back,eff,LW}$ are independent of the value chosen for T because G_5 and G_6 are each proportional to σT^4.

Given the assumptions that each surface is perfectly diffuse and gray, the total, effective hemispherical emittance and absorptance values will also be equal; that is,

$$\varepsilon_{k,eff,LW} = \alpha_{k,eff,LW} . \tag{14}$$

The implication of Equation 14 is that Equation 12 and Equation 13 can be used as a third method for calculating the effective longwave absorptance for side k. This was done, and the results were used to confirm consistency of the computer code.

Effective Longwave Reflectance ($\rho_{k,eff,LW}$)

The fraction of the imposed irradiance, G_k, that is apparently reflected by the k surface of the shading layer, $\rho_{k,eff,LW}$, can be determined from an energy balance on the blind enclosure. The rate of energy supplied to the enclosure is $A_k G_k$. The rate of reflection can be determined from the rate energy leaves the blind enclosure through side k, which is the product of the irradiance on the opening surface, G_5 (front) or G_6 (back), and the area over which it is incident, A_k. Thus for the front side,

$$\rho_{front,eff,LW} A_k G_{front} = A_5 G_5 , \tag{15}$$

and for the back side,

$$\rho_{back,eff,LW} A_k G_{back} = A_6 G_6 . \tag{16}$$

Rearranging for the front side, with $A_5 = A_k$,

$$\rho_{front,eff,LW} = \frac{G_5}{G_{front}} , \tag{17}$$

and, for the back side, with $A_6 = A_k$,

$$\rho_{back,eff,LW} = \frac{G_6}{G_{back}} . \tag{18}$$

Equation 17 and Equation 18 represent methods for determining the effective longwave reflectance of the shading layer. It should be noted that $\rho_{k,eff,LW}$ is independent of the magnitude of G_k because each of G_5 and G_6 is proportional to G_k.

Effective Longwave Reflectance—Results

Figure 5 shows $\rho_{front,eff,LW}$ as a function of slat angle for different w/s ratios and $\varepsilon_{top} = 0.8$ and $\varepsilon_{bottom} = 0.7$. The reflectance of the venetian blind layer increases as the slat angle departs from $\phi = 0$ because more of the irradiance, G_k, is intercepted by the slats. Also note that for $w/s \geq 1$ and $\phi = \pm 90°$, $\rho_{f,eff,LW}$ and the reflectance of the slat surface facing the front, $(1 - \varepsilon_{top})$ or $(1 - \varepsilon_{bottom})$, must be equal. This is expected because the front surface of the shading layer will be entirely composed of the exposed slat surface. Of course, the same relation exists between the back-side effective reflectance and the reflectance of the slat itself.

Effective Longwave Transmittance ($\tau_{k,eff,LW}$)

The fraction of the imposed irradiance, G_k, that is transmitted by the shading layer, $\tau_{k,eff,LW}$, can be determined from an energy balance on the blind enclosure. The rate of energy supplied to the enclosure will be the product of A_k and G_k. The effective rate of transmission can be determined from the rate of energy that leaves the blind enclosure through the side

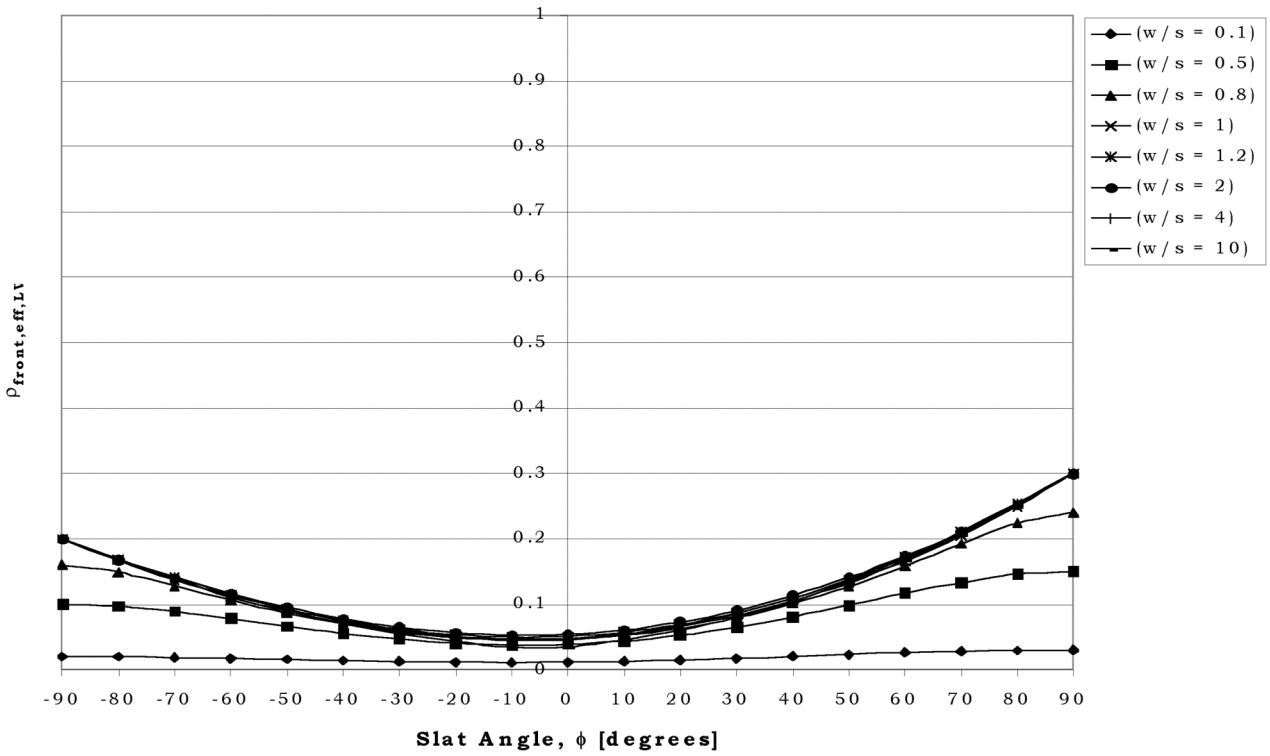

Figure 5 *Front effective longwave reflectance as a function of slat angle for various* w/s *ratios,* $\varepsilon_{top} = 0.8$, *and* $\varepsilon_{bottom} = 0.7$.

opposite k, which will be A_6G_6 (FEP) or A_5G_5 (BEP). Thus, for the front side,

$$\tau_{front,eff,LW} = \frac{G_6}{G_{front}}, \tag{19}$$

and, for the back side,

$$\tau_{back,eff,LW} = \frac{G_5}{G_{back}}. \tag{20}$$

Equation 19 and Equation 20 represent methods for determining the effective longwave transmittance of the shading layer for the front and back sides. It should be noted that, as mentioned for previous cases, $\tau_{k,eff,LW}$ is independent of the value chosen for G_k. Also, on the basis of second law thermodynamic arguments, the front and back effective longwave transmittances must be equal. Equations 19 and 20 and this requirement were used to double-check the consistency of the computer code.

Effective Longwave Transmittance—Results

Figure 6 shows $\tau_{eff,LW}$ as a function of slat angle for different w/s ratios and $\varepsilon_{top} = 0.8$ and $\varepsilon_{bottom} = 0.7$. Note that for $w/s \geq 1$ and $\phi = 90°$, the value of the effective transmittance is always zero. This should be expected because the surface of the shading layer will be composed entirely of the slat surface, which is opaque to longwave radiation. For $w/s < 1$, the effective transmittance is equal to $1 - w/s$, which is equal to the fraction of the blind layer that remains unobstructed. Although large w/s values are not practical, it is instructive to observe that as the w/s ratio is increased to values much greater than unity, the effective transmittance approaches zero, even when the blind is in the open position ($\phi = 0$) because radiation that enters the cavity is reflected diffusely from the slat surfaces and is largely unable to escape from the far-side cavity opening.

DISCUSSION OF EFFECTIVE LONGWAVE PROPERTIES

The effective properties of the blind layer are a function of w, s, ϕ, ε_{top}, and ε_{bottom}. Figures 4, 5, and 6 demonstrate the dependence of each effective longwave radiative property on w, s, and ϕ. The effective transmittance displays a strong dependence on the w/s ratio, as shown in Figure 6. This should be expected because the w/s ratio dictates how much radiation will be transmitted through the blind layer without interaction with the blind slats. From a radiation balance on the blind enclosure, the sum of the effective absorptance, reflectance, and transmittance must be equal to unity. Since the properties are connected in this way, if one property shows a dependence on the w/s ratio and slat angle, then at least one other property will exhibit a related dependence. From Figure 4, it is seen that the effective absorptance also exhibits a strong dependence on the w/s ratio. This is due to the choice of highly absorptive

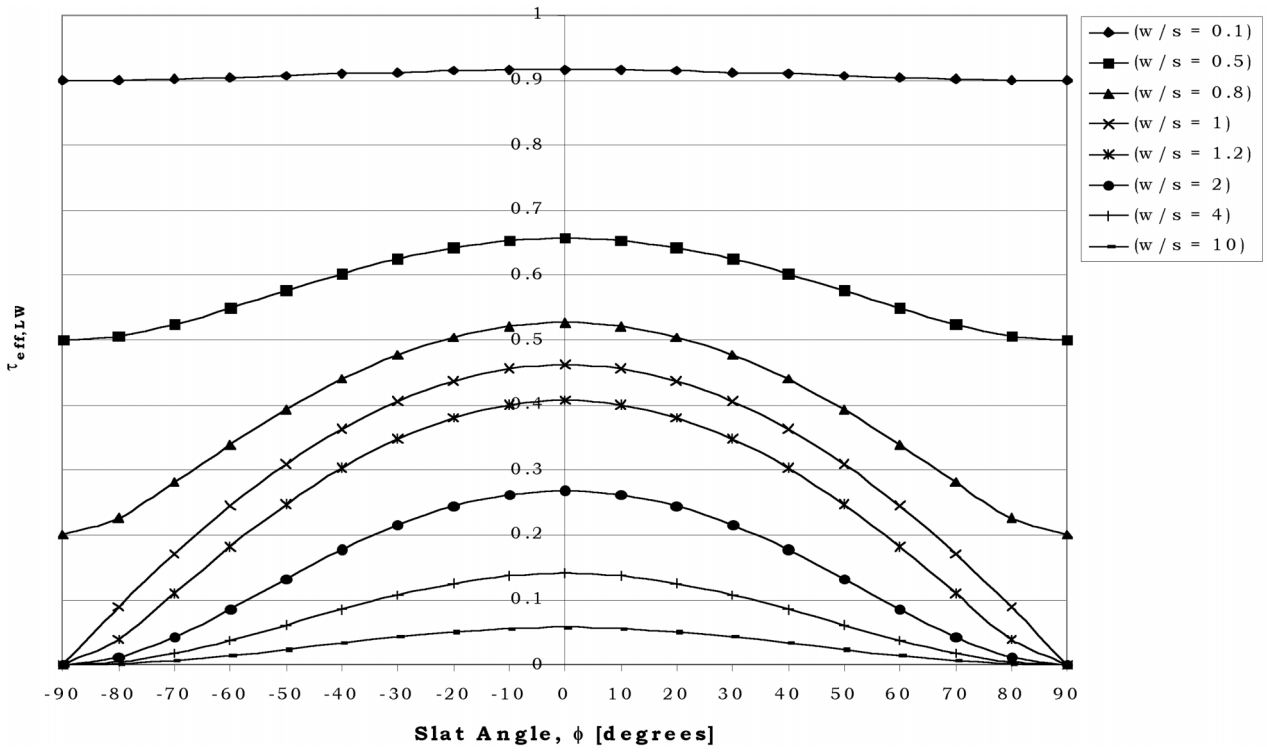

Figure 6 *Front effective longwave transmittance as a function of slat angle for various* w/s *ratios and* $\varepsilon_{top} = 0.8$ *and* $\varepsilon_{bottom} = 0.7$.

blind slats. Most of the radiation not transmitted directly through the blind enclosure is absorbed by the slat surfaces. This also explains why the effective reflectance is only weakly dependent on the *w*/*s* ratio, especially for situations where the slat width is greater than the slat spacing. If the blind slats were highly reflective, the *w*/*s* ratio dependence of the absorptance and reflectance would be reversed.

To demonstrate the effective properties' dependence on the slat emissivity, two cases were examined. Case 1 entails highly absorptive slats ($\varepsilon_{top} = 0.8$ and $\varepsilon_{bottom} = 0.7$), and case 2 entails highly reflective slats ($\varepsilon_{top} = 0.2$ and $\varepsilon_{bottom} = 0.1$). Figure 7 illustrates, for the common arrangement of $w/s = 1$, how the front effective properties vary for highly absorptive (solid symbols) and reflective (open symbols) slats. Note that the effective absorptance and reflectance are highly sensitive to changes in the slat emissivities (ε_{top} and ε_{bottom}), especially for higher slat angles. The effective transmittance has a milder sensitivity to changes in the slat emissivity, especially for higher slat angles, as expected.

Flat Slat Model vs. Curved Slat Model

In order to gain an understanding of the error introduced by the "flat slat" assumption, a curved slat model was created. The effective longwave radiative properties for the curved slat model can be calculated using the same procedure used in the flat slat model with view factors being determined to account for slat surface self-viewing. The degree of slat curvature is quantified using its radius of curvature, r_c, as defined in Figure 8. The inset of Figure 8 visually depicts the radius of slat curvature as a function of the slat radius-to-spacing ratio, r_c/s.

Results of the curved slat and flat slat models are compared in Figures 9 ($\phi = 0$) and 10 ($\phi = 45°$). In both figures, the discrepancy in the front effective optical property values is plotted as a function of the r_c/s ratio. Specifically, discrepancies in values of $\tau_{front,eff,LW}$, $\rho_{front,eff,LW}$, and $\alpha_{front,eff,LW}$ are shown for $w/s = 0.6$ and $w/s = 1.2$.

In each of Figures 9 and 10, the discrepancy between the various effective longwave properties calculated using the flat and curved slat models is shown on the vertical axis. This discrepancy is most strongly dependent on the *w*/*s* ratio and weakly dependent on the slat emissivities (ε_{top}, ε_{bottom}) and the slat angle, ϕ. In each case, the lower and uppermost curves correspond to effective absorptance and transmittance values, respectively, for the larger, and more realistic, *w*/*s* ratio ($w/s = 1.2$). Curves for the smaller *w*/*s* ratio ($w/s = 0.6$) are tightly grouped, to the extent that it is difficult to distinguish one curve from another, and the corresponding discrepancy values are very small. This is to be expected because at high *w*/*s* ratios, the interaction of the slats with incident radiation will be greater and the self-viewing nature of individual slats will be more pronounced. Assuming that most slats have a radius of curvature such that $r_c/s \approx 2$, errors of approximately 0.01

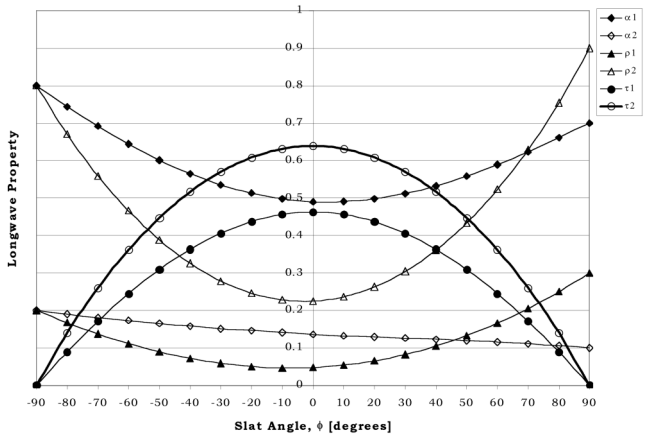

Figure 7 *Front effective properties for absorptive (solid symbols with $\varepsilon_{top} = 0.8$ and $\varepsilon_{bottom} = 0.7$) and reflective slats (hollow symbols with $\varepsilon_{top} = 0.2$ and $\varepsilon_{bottom} = 0.1$) as a function of slat angle.*

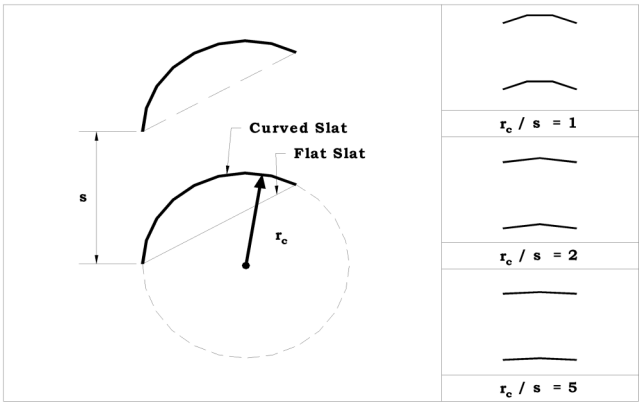

Figure 8 *Curved slat and flat slat geometry.*

may be expected in the effective absorptance and transmittance values as a result of the flat-slat simplification. This error may be unacceptably large if highly curved slats are being analyzed. Of course, the discrepancy between the two models approaches zero as the radius of curvature is increased.

Four-Surface vs. Six-Surface Enclosure Model

The effective property models previously discussed are based on a six-surface enclosure. For cases where the slats do not overlap in the closed position ($w \leq s$), the six-surface enclosure reduces to a four-surface enclosure. For cases where slat overlap is possible ($w > s$), six surfaces are required to model the enclosure.

Figure 11 compares the front effective properties determined using a four-surface and six-surface model with $w/s = 1.2$ ($\varepsilon_{top} = 0.8$, $\varepsilon_{bottom} = 0.7$) and shows that for high slat angles, the effective properties determined using the four-surface and six-surface models differ. In particular, the transmittance determined using the four-surface enclosure model does not approach zero with the blind in the closed position. This occurs because the radiant analysis is based on the assumption that the irradiance of the ith surface, G_i, is uniform over the entire area, A_i. However, the slat surface facing the front opening will be partially blocked by the adjacent slat. In the four-surface model, with uniform slat irradiation, the overlapped portion of the slat will be treated as being uniformly irradiated as well. Since this overlapped portion sees the overlapped portion of the adjacent slat surface, and the adjacent slat surface sees the back opening, a false transmittance results. By modeling the enclosure with six surfaces, the slat surface facing the front opening is split in two, with the exposed surface being irradiated and the overlapped surface treated as being completely shaded. Using the six-surface model, there is no false transmittance produced.

CONCLUSIONS

The effective longwave radiative property models described can be incorporated in a one-dimensional center-glass heat transfer analysis of a glazing system with a venetian blind, where the venetian blind is treated as a shading layer in a series of glazing layers.

The effective longwave radiative property models for a venetian blind shading layer are based on a spatially representative six-surface enclosure, which is bounded by two adjacent slats and the front and back openings to the blind. The longwave radiation exchange between surfaces in the enclosure is modeled, assuming each surface is a diffuse emitter/reflector, each surface is uniformly irradiated, and each surface is gray with respect to longwave radiation. The effective longwave absorptance, reflectance, and transmittance are determined by introducing an external irradiance on one opening of the enclosure and solving for the enclosure surface radiosities and irradiances. The resulting expressions for the effective longwave radiative properties are functions of the hemispherical longwave emissivity of each slat surface, the slat angle, ϕ, slat width, w, and slat spacing, s. The behavior of each property with respect to slat emissivity, ϕ, w, and s is as expected.

ACKNOWLEDGMENTS

This research was supported by Natural Sciences and Engineering Research Council.

REFERENCES

Hollands, K.G.T., J.L. Wright, and C.G. Granqvist. 2001. Glazings and coatings. *Solar Energy—The State of the Art—ISES Position Papers*, Chapter 2, pp. 29-50.

ISO. 2000. ISO/DIS 15099. Thermal performance of windows, doors, and shading devices—Detailed calcula-

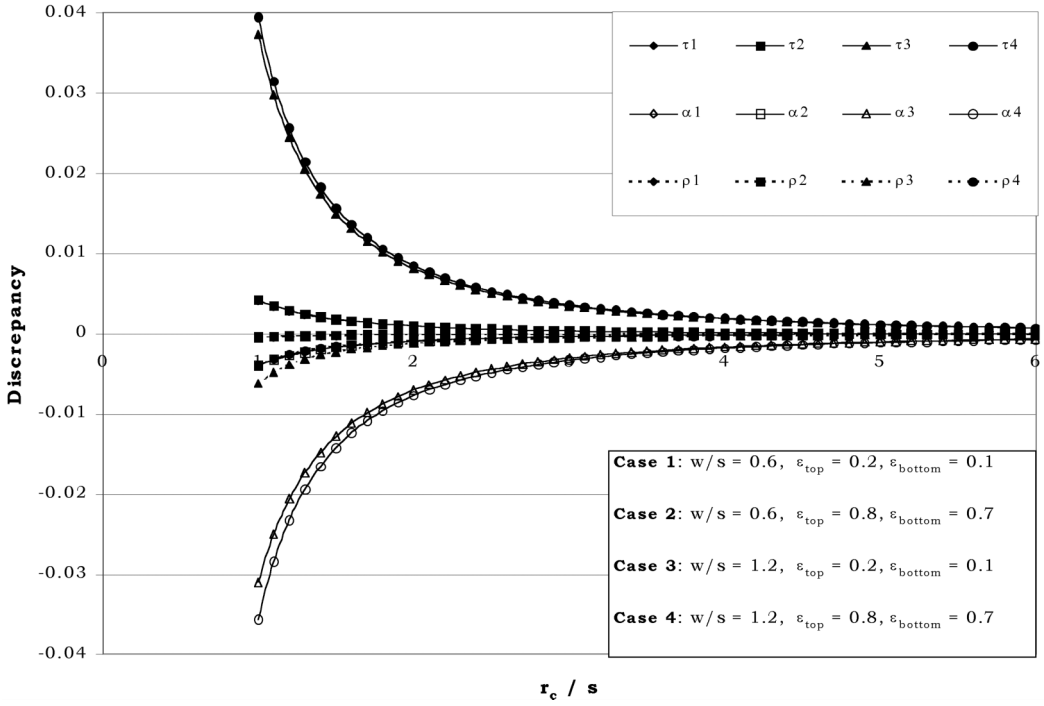

Figure 9 *Discrepancy in front effective longwave properties between curved and flat slat models as a function of* r_c/s *for* $\phi = 0°$.

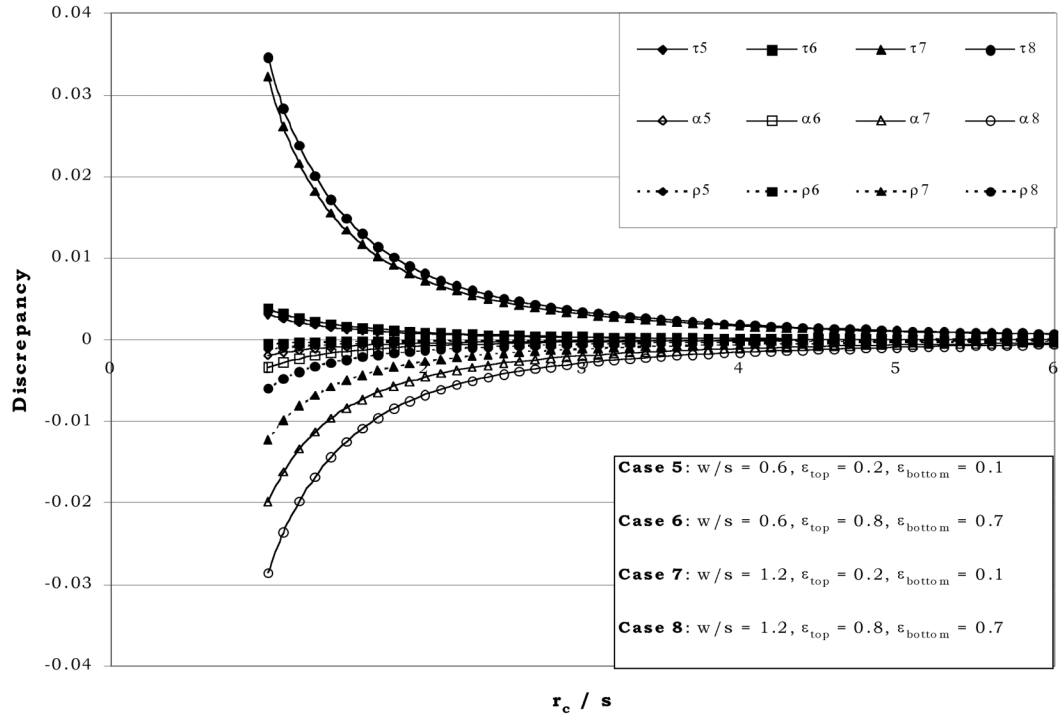

Figure 10 *Discrepancy in front effective longwave properties between curved and flat slat models as a function of* r_c/s *for* $\phi = 45°$.

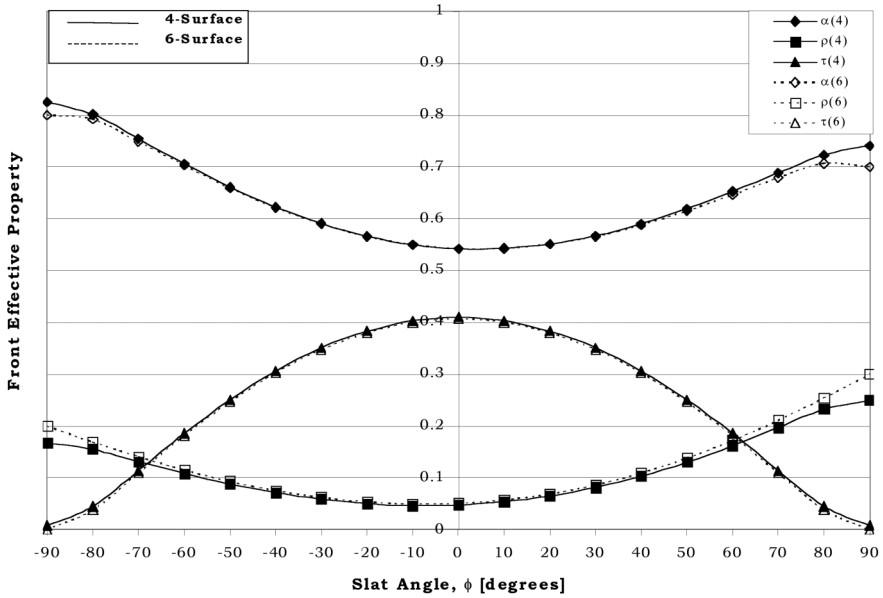

Figure 11 *Comparison of effective properties using four-surface and six-surface models with slat overlap (*w/s *= 1.2,* ε_{top} *= 0.8, and* ε_{bottom} *= 0.7).*

tions. The International Organisation for Standardisation.

Klems, J.H. 1994a. A new method for predicting solar heat gain of complex fenestration systems: I. Overview and derivation of the matrix layer calculation. *ASHRAE Transactions* 100(1): 1065-1072.

Klems, J.H. 1994b. A new method for predicting solar heat gain of complex fenestration systems: II. Detailed description of the matrix layer calculation. *ASHRAE Transactions* 100(1): 1073-1086.

Klems, J.H. 2002. Solar heat gain through fenestration systems containing shading: Procedures for estimating performance from minimal data. *ASHRAE Transactions* 109(1).

Rheault, S., and E. Bilgen. 1989. Heat transfer analysis in an automated venetian blind system. *Journal of Solar Energy*, Vol. 111 (Feb.), pp. 89-95.

Siegel, R., and J.R. Howell. 1992. *Thermal Radiation Heat Transfer*. New York: McGraw Hill.

Wright, J.L. 1998. Calculating center-glass performance indices of windows. *ASHRAE Transactions* 104(1).

DISCUSSION

Charlie Curcijn, Senior Research Fellow, University of Massachusetts, Amherst, Mass.: Was this model verified vs. ISO 15099 model?

John Wright: We compared effective longwave properties against a small number of sample values included in the ISO 15099 document and the agreement was very good. We were curious about this because they divide each slat into five subsurfaces whereas we use only one or two surfaces per slat. The convection models described in this paper are relatively crude and were used as a starting point to compare against some of our own heat transfer measurements. As we complete additional heat transfer measurements, in particular using low-e coatings, and as we examine the results of numerical modelling we will be formulating a more realistic convection model. At that stage we will be making comparisons with the European software. It should be remembered that the heat transfer analysis is almost a secondary consideration because the key information is the Solar Heat Gain Coefficient. We have developed a model for solar gain with venetian blinds and the corresponding technical paper is being prepared.

Tom McHugh, HMG, Fair Oaks, Calif.: Convection models: (1) Model as if no blinds? (2) Model as two convective loops? (3) Curvature of V-factor with respect to slat angle only to radiative effects?